

Bandwidth enhancement phenomenon of a high-speed GaAs–AlGaAs based untraveling carrier photodiode with an optimally designed absorption layer at an 830 nm wavelength

Jin-Wei Shi, Yu-Tai Li, Ci-Ling Pan, M. L. Lin, Y. S. Wu, W. S. Liu, and J.-I. Chyi

Citation: *Applied Physics Letters* **89**, 053512 (2006); doi: 10.1063/1.2267088

View online: <http://dx.doi.org/10.1063/1.2267088>

View Table of Contents: <http://scitation.aip.org/content/aip/journal/apl/89/5?ver=pdfcov>

Published by the [AIP Publishing](#)

Articles you may be interested in

The mechanism of the photoresponse blueshifts for the n-type conversion region of n + -on- p Hg 0.722 Cd 0.278 Te infrared photodiode

J. Appl. Phys. **107**, 044513 (2010); 10.1063/1.3298476

Beryllium compensation doping of In As Ga Sb infrared superlattice photodiodes

Appl. Phys. Lett. **91**, 143507 (2007); 10.1063/1.2795086

High quality of 830 nm material grown by solid source molecular beam epitaxy for laser device printing applications

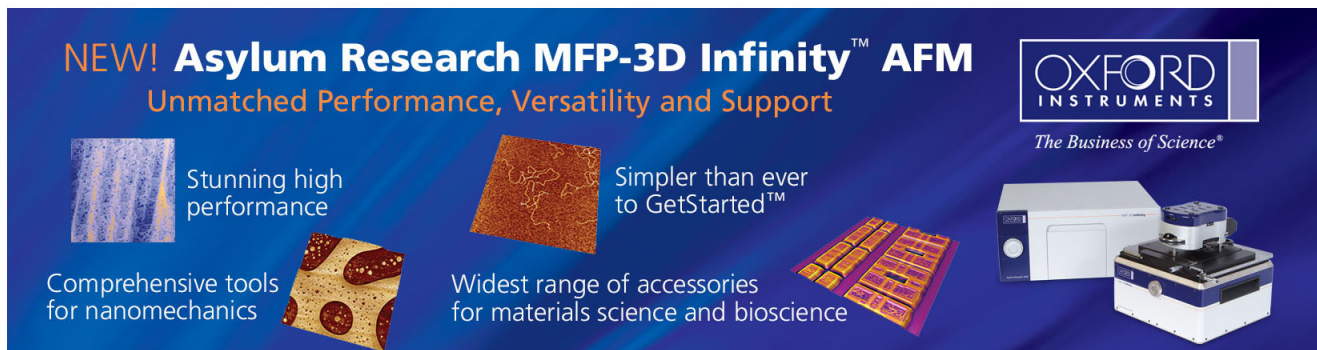
J. Vac. Sci. Technol. B **25**, 926 (2007); 10.1116/1.2718963

Rectification and intrinsic photocurrent of Ga As Si photodiodes formed with pulsed-laser deposition at 1064 nm

Appl. Phys. Lett. **87**, 151115 (2005); 10.1063/1.2093942

Passivation of InAs (GaIn) Sb short-period superlattice photodiodes with 10 μm cutoff wavelength by epitaxial overgrowth with Al x Ga 1 - x As y Sb 1 - y

Appl. Phys. Lett. **86**, 173501 (2005); 10.1063/1.1906326



NEW! Asylum Research MFP-3D Infinity™ AFM
Unmatched Performance, Versatility and Support

OXFORD INSTRUMENTS
The Business of Science®

Stunning high performance

Simpler than ever to GetStarted™

Comprehensive tools for nanomechanics

Widest range of accessories for materials science and bioscience

Asylum Research

Bandwidth enhancement phenomenon of a high-speed GaAs–AlGaAs based untraveling carrier photodiode with an optimally designed absorption layer at an 830 nm wavelength

Jin-Wei Shi^{a)}

Department of Electrical Engineering, National Central University, Taoyuan, 320 Taiwan, Republic of China

Yu-Tai Li and Ci-Ling Pan

Institute of Electro-Optical Engineering, National Chiao Tung University, Hsinchu, 300 Taiwan, Republic of China

M. L. Lin, Y. S. Wu, W. S. Liu, and J.-I. Chyi

Department of Electrical Engineering, National Central University, Taoyuan, 320 Taiwan, Republic of China

(Received 7 April 2006; accepted 19 June 2006; published online 3 August 2006)

In this letter, the authors introduce a GaAs/AlGaAs based untraveling carrier photodiode (UTC-PD) for a wavelength of around 830 nm. There is significant bias- and output-current-dependent bandwidth enhancement phenomena observed with this device. According to their microwave and optical-to-electrical measurement results, such distinct phenomena can occur under a much lower current density ($0.3 \text{ mA}/\mu\text{m}^2$ vs $0.05 \text{ mA}/\mu\text{m}^2$) than previously reported for InP–InGaAs UTC-PDs. This can be attributed to the self-induced field in the absorption region, made possible due to the optimized p -type doping profile. © 2006 American Institute of Physics. [DOI: 10.1063/1.2267088]

Due to the maturity of high-performance optical light sources with wavelengths around 800 nm, several photomixing experiments for terahertz wave generation¹ and ultrafast optoelectronic measurement or sampling² in this wavelength regime have already been done. Low-temperature-grown GaAs (LTG GaAs) based photodetectors are a promising choice for those applications.^{1,3} Recently, a standard kit and system for terahertz spectroscopy, composed of a LTG-GaAs based terahertz emitter/receiver, has been made commercially viable.⁴ However, compared with the typical GaAs based p - i - n photodiodes (PDs), the LTG-GaAs based photodetectors still suffer from the problem of decreased external efficiency due to the existence of recombination centers in the photoabsorption layer.³ InGaAs–InP based untraveling carrier photodiode (UTC-PD) structures⁵ are another attractive choice for high-power, high-speed applications.⁵ However, in the case of InP based UTC-PDs under 0.8 μm wavelength excitation, the incident photons produce enough photon energy to induce absorption in the whole epilayer structure. Thus in this work, we develop a high-speed GaAs/AlGaAs based UTC-PD, which is composed of a GaAs based p -type photoabsorption layer and an $\text{Al}_{0.15}\text{Ga}_{0.85}\text{As}$ based collector layer to avoid the undesired photoabsorption that occurs in the collector layer under 800 nm wavelength excitation.

The conceptual band diagram of the demonstrated UTC-PD device is shown in Fig. 1. The inset to Fig. 1 shows the top view of the fabricated device. As shown in Fig. 1, we utilize a graded p -type doping profile in the GaAs based photoabsorption layer, with a total thickness of 160 nm, to accelerate the photogenerated electrons.⁶ When compared to

the previous work on InP–InGaAs based UTC-PDs,^{5–7} it can be seen that our structure has a more abrupt p -type doping gradient slope, which induces a much stronger built-in electric field to accelerate the electrons. The collector layer consists of a n -type doped ($8 \times 10^{16} \text{ cm}^{-3}$)⁷ $\text{Al}_{0.15}\text{Ga}_{0.85}\text{As}$ layer, 200 nm in thickness and with a band gap of around 1.61 eV.⁸ This enables one to avoid the undesired photoabsorption process that occurs around 800 nm wavelength excitation. A n^+ doped ($5 \times 10^{18} \text{ cm}^{-3}$) $\text{Al}_{0.15}\text{Ga}_{0.85}\text{As}$ cliff layer was inserted between the collector layer and the absorption layer.⁶ As shown in the inset, we adopted the structure of an edge-coupled waveguide photodiode and the n^+ and p^+ doped ($5 \times 10^{19} \text{ cm}^{-3}$) $\text{Al}_{0.15}\text{Ga}_{0.85}\text{As}$ layers, which surrounded the active collector and absorption layers, serve as the optical cladding layers. Details of the device fabrication processes and geometric structure have already been given in our previous work.⁹

In order to characterize the dynamic performance of our device under continuous-wave (cw) operation, we utilized a heterodyne-beating system and a lightwave-component-analyzer (LCA) system to measure the frequency responses and scattering (S) parameters of the devices. The LCA system was composed of a 65 GHz vector-network analyzer, with a well-calibrated electrical-to-optical modulator with an electrical bandwidth of around 30 GHz, and a tunable semiconductor laser, which had a center wavelength fixed at 830 nm. Figure 2 shows the $f_{3 \text{ dB}}$ bandwidths of the UTC-PD with a $60 \mu\text{m}^2$ active area measured under different optical pumping powers, different reverse bias voltages, and a fixed 50 Ω load. The inset shows the frequency responses of a similar device measured under different optical pumping powers (2, 8, and 15 mW) and a fixed reverse bias voltage (–5 V). The maximum output photocurrent ($\sim 1 \text{ mA}$) of the devices is limited by the maximum available optical power

^{a)} Author to whom correspondence should be addressed; FAX: +886-3-425 5830; electronic mail: jwshi@ee.ncu.edu.tw

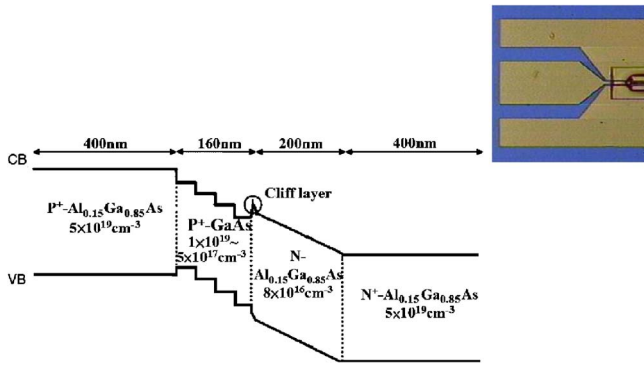


FIG. 1. Conceptual band diagram of the demonstrated UTC-PD. The inset shows the top view of the fabricated device, which has an edge-coupled waveguide photodiode structure.

of the measurement system. The poor responsivity of our primarily demonstrated device is limited by the poor coupling efficiency between a narrow waveguide with a 2 μm width and the injected optical signal with an ~5 μm beam radius. Significant bandwidth enhancement phenomena, especially under a high reverse bias voltage (-5 V) and high output photocurrent (~1 mA), can be observed. However, under low reverse bias voltages (-1 and -3 V), such phenomena are ambiguous. The measurement results shown in Fig. 2 exhibit a very different trend from the reported space-charge-screening effect,⁹ which was usually observed for the case of photodiode under high-power operation and should not exhibit a significant bandwidth enhancement with an increase in the optical pumping power. The overall bandwidth of a PD is determined by the carrier transport time (1/f_t) and the RC time constant (1/f_{RC}). The net 3 dB bandwidth (f_{3 dB}) can be approximated as follows:¹⁰

$$\frac{1}{f_{3\text{ dB}}^2} = \frac{1}{f_{RC}^2} + \frac{1}{f_t^2} = (2\pi RC)^2 + \frac{1}{f_t^2}, \quad (1)$$

where R is the sum of the parasitic resistance and the load resistance (50 Ω) and C is the total capacitance. In order to study which factor (1/f_t or 1/f_{RC}) dominates the observed distinct dynamic performance, we measured the optical-to-electrical (O-E) bandwidth (S₂₁) and microwave reflection

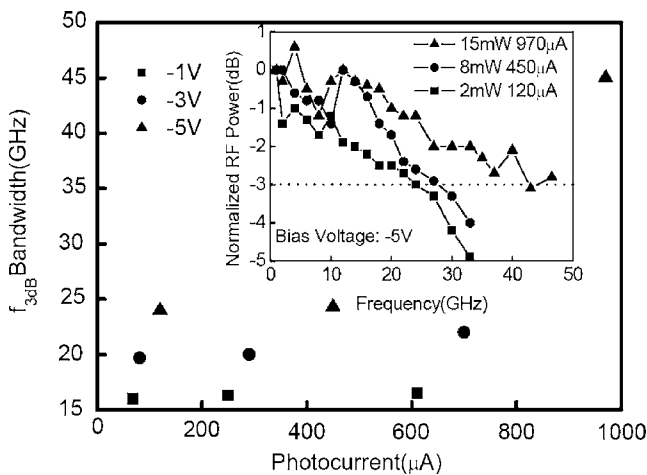


FIG. 2. f_{3 dB} bandwidths of the UTC-PD measured under different output photocurrents and reverse bias voltages. The inset shows the frequency responses of UTC-PD measured under different optical pumping powers (2, 8, and 15 mW) but with a fixed reverse bias voltage (-5 V).

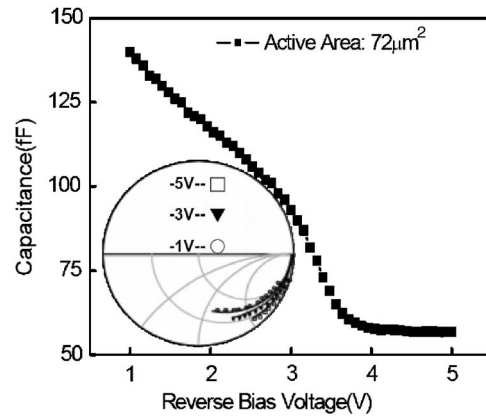


FIG. 3. Extracted values of capacitance vs reverse bias voltage. The UTC-PD has a 72 μm² active area. The inset shows the measured frequency responses (20 MHz–20 GHz) of the bias-dependent (-1, -3, and -5 V) S₂₂ parameters on the Smith chart.

coefficients (S₂₂) using the LCA system. The inset to Fig. 3 shows the frequency responses (from 20 MHz to 20 GHz) for bias-dependent S₂₂ parameters on the Smith chart. By utilizing the measured S₂₂ parameters, we can further extract the values of C. Figure 3 shows the extracted C versus reverse bias voltages (V). When the bias is -5 V, the value of C (~57 fF) is close to the ideal junction capacitance (~42 fF) with additional parasitic capacitance (~15 fF). According to the C-V and S₂₂ measurement results, we can conclude that the significant bias-dependent speed performance is originated from the depletion of collector layer when the reverse bias voltage is larger than -3.5 V. The bandwidth enhancement under low bias voltages (-1 and -3 V) is less apparent, due to serious RC-bandwidth limitation. The observed bandwidth enhancement with increasing output current, which has also been reported for the InP-InGaAs based UTC-PDs, has been attributed to a self-induced field in the absorption layer,^{5,7} a reduction in the ac capacitance,¹¹ or velocity overshooting of electrons in the collector layer.¹¹ In our case, velocity overshooting in the collector can be ignored, because the electric field (at a bias of -5 V) in the collector layer (~250 kV/cm) is much larger than the critical field (~5 kV/cm).^{8,12} The reported reductions in the ac capacitance of the UTC-PD should be accompanied by a significant variation in the measured S₂₂ parameter when the photocurrent is increased under a fixed bias.¹¹ Figures 4(a) and 4(b) show the measured frequency responses of S₂₁ and S₂₂ under a fixed reverse bias voltage (-5 V) and different output photocurrents. The active area of the measured device is around 72 μm². It can be seen that

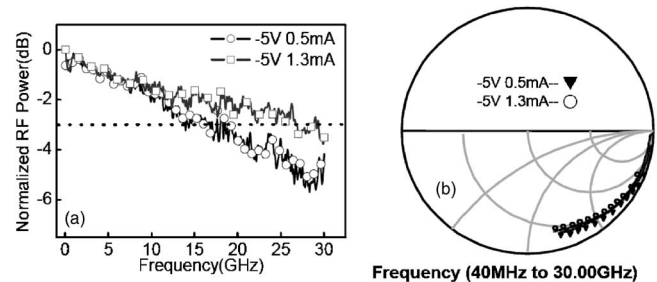


FIG. 4. Measured frequency responses of S₂₁ (a) and S₂₂ (b) parameters of UTC-PD under different output photocurrents but at a fixed reverse bias voltage.

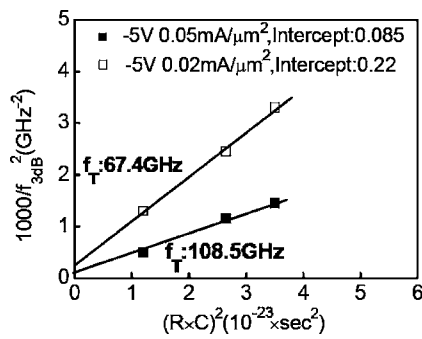


FIG. 5. Extracted $(R \times C)^2$ vs measured $(1000/f_{3\text{dB}}^2)$ of UTC-PDs with three different active areas (56, 72, and $92 \mu\text{m}^2$) under different output photocurrent densities (0.02 and $0.05 \text{ mA}/\mu\text{m}^2$) and a fixed reverse bias voltage (-5 V). The extrapolated f_t 's are also labeled.

significant bandwidth enhancement phenomenon still exists ($\sim 17 \text{ GHz}$ vs $\sim 27 \text{ GHz}$); however, the S_{22} parameters measured under different output photocurrents are similar. We can thus conclude that the self-induced field and the corresponding reduction of electron transit time in the p -type absorption layer dominate the observed bandwidth enhancement phenomena. The self-induced field is proportional to the output current density.⁵ We can use Eq. (1) and the RC-limited bandwidths of devices with different active areas under a fixed output current density to extract the transit-time-limited bandwidth (f_t).¹⁰ In order to accurately obtain the effective absorption area (length) and current density of our edge-coupled structure, we measured device responsivity with different absorption lengths. The measurement results indicate that the effective length necessary for complete photoabsorption is around $12 \mu\text{m}$. Figure 5 shows the $(RC)^2$ vs $(1000/f_{3\text{dB}}^2)$ values. There were three different active areas under two different output photocurrent densities and a fixed reverse bias voltage (-5 V). We can clearly see that, when the photocurrent density reaches $0.05 \text{ mA}/\mu\text{m}^2$, the extrapolated f_t increases from 67.4 to 108.5 GHz. These results indicate that the total transit delay time can be reduced from 2.36 to 1.47 ps. If we assume a saturated electron drift velocity ($\sim 1 \times 10^5 \text{ m/s}$) with a collector thickness of 200 nm, the calculated collector signal delay will be around 1 ps, which leaves 1.36 and 0.47 ps as the absorption layer transit times (τ_A) under a low and high current density, respectively. By using the extracted τ_A under low current operation and the τ_A formulas,⁵ we can now obtain the value of the minority electron diffusion coefficient (D_n), which is around $100 \text{ cm}^2/\text{s}$ and consistent with the typical value in the p -type GaAs layer.⁸ On the other hand, for high current operation, we can assume that there is electron drift in the absorption

layer and the estimated drift velocity is around $3 \times 10^7 \text{ cm/s}$. This value is also close to the overshoot velocity of electron in the GaAs.⁸ Our structure can achieve a similar increased bandwidth value ($\sim 10 \text{ GHz}$) compared to the reported InP–InGaAs UTC-PD,⁷ but under a much lower current density ($0.3 \text{ mA}/\mu\text{m}^2$ vs $0.05 \text{ mA}/\mu\text{m}^2$). This result could possibly be due to the fact that the built-in electric field ($1.5\text{--}30 \text{ kV/cm}$) in our absorption layer is much stronger than that of the reported UTC-PDs, which ranges between 0.43 and 1.7 kV/cm .⁷ This means that smaller self-induced field (current density) will be required to accelerate an electron to near its overshoot velocity. The demonstrated technique has the potential to widen the linear operational regime of UTC-PDs, because the 3 dB bandwidth of the device can be enhanced and maintained, even from a small output photocurrent, until the saturation phenomenon occurs in the high current regime.

We develop and discuss a GaAs/AlGaAs based UTC-PD under an 830 nm wavelength operation. According to the O-E measurement results, there is significant bandwidth enhancement, due to the self-induced field in the absorption layer and the depletion of the collector layer. The demonstrated device has the potential to increase the linear operating regime of UTC-PDs and serve as a terahertz emitter by properly downscaling the active area of device under wavelengths around 800 nm.

¹S. M. Duffy, S. Verghese, K. A. McIntosh, A. Jackson, A. C. Gossard, and S. Matsuura, IEEE Trans. Microwave Theory Tech. **49**, 1032 (2001).

²K. J. Weingarten, M. J. W. Rodwell, and D. M. Bloom, IEEE J. Quantum Electron. **24**, 198 (1988).

³D. Lasaosa, J.-W. Shi, D. Pasquariello, K.-G. Gan, M.-C. Tien, H.-H. Chang, S.-W. Chu, C.-K. Sun, Y.-J. Chiu, and J. E. Bowers, IEEE J. Sel. Top. Quantum Electron. **10**, 728 (2004).

⁴The kit is supported by EKSPLA Corp. Lithuania, www.ekspla.com

⁵H. Ito, S. Kodama, Y. Muramoto, T. Furuta, T. Nagatsuma, and T. Ishibashi, IEEE J. Sel. Top. Quantum Electron. **10**, 709 (2004).

⁶N. Shimizu, N. Watanabe, T. Furuta, and T. Ishibashi, IEEE Photonics Technol. Lett. **10**, 412 (1998).

⁷N. Li, X. Li, S. Demiguel, X. Zheng, J. C. Campbell, D. A. Tulchinsky, K. J. Williams, T. D. Isshiki, G. S. Kinsey, and R. Sudharsanan, IEEE Photonics Technol. Lett. **16**, 864 (2004).

⁸M. Levinshtein, S. Rumyantsev, and M. Shur, Handbook Series on Semiconductor Parameters (World Scientific, Singapore, 1996), Vol. 2, p. 64.

⁹J.-W. Shi, H.-C. Hsu, F.-H. Huang, W.-S. Liu, J.-I. Chyi, Ja-Yu Lu, Chi-Kuang Sun, and Ci-Liang Pan, IEEE Photonics Technol. Lett. **17**, 1722 (2005).

¹⁰L. Zheng, X. Zhang, Y. Zeng, S. R. Tatavarti, S. P. Watkins, C. R. Bolognesi, S. Demiguel, and J. C. Campbell, IEEE Photonics Technol. Lett. **17**, 651 (2005).

¹¹Y.-S. Wu, J.-W. Shi, and P.-H. Chiu, IEEE Photonics Technol. Lett. **18**, 938 (2006).

¹²A. Das and M. Lundstrom, IEEE Electron Device Lett. **12**, 335 (1991).